small methods
www.small-methods.com

Broadband Photodetector Based on Inorganic Perovskite $CsPbBr_3$/GeSn Heterojunction

*Hui Cong, Xinbo Chu, Fengshuo Wan, Zema Chu, Xiaoyu Wang, Yao Ma, Jizhong Jiang, Liang Shen, Jingbi You, and Chunlai Xue**

Photodetectors with broadband response spectrum have attracted great interest in many application areas such as imaging, gas sensing, and night vision. Here, a high performance broadband photodetector is demonstrated with inorganic perovskite $CsPbBr_3$/GeSn heterojunction, detection range can be covered from 450 to 2200 nm. The responsivity of heterojunction device can achieve as high as 129 mA W^{-1} under illuminated light of 532 nm, which is 4.92 times larger than that of a GeSn based device. As the $CsPbBr_3$ can also act as anti-reflective coating for infrared wavelength, the infrared band responsivity at wavelength of 2200 nm can also be raised by 1.42 times. In addition, the device with all inorganic components is showed good stability, while keeping in the dry environment, the device can sustain its 90% original after 550 h storage. These results show the inorganic perovskite/GeSn heterojunction device is of great potential in broadband photodetection with high responsivity.

1. Introduction

Photodetectors with broadband response spectrum are able to access more information than photodetectors operating at a narrow spectral region, which can be widely used in remote sensing, imaging, data communication, gas sensing, night vision, and so on.[1–3] In recent years, photodetectors with detection range from visible (Vis) light to infrared (IR) have attracted great interests.[4–7] As the detection range is mainly determined by the band gap of the absorption layer, it is difficult to realize a broadband detection with one single material. For example, the spectral response for a commercial Si photodiode is between the wavelength from 400 to 1100 nm and the maximum responsivity is located near 1000 nm.[8] Thanks to the mature fabrication process, Si photodiodes have been widely used, but its application is limited by lack of response in range of short-wave-infrared (SWIR) and the low responsivity in visible light. Photodetectors with active layers of traditional semiconductor materials, such as germanium (Ge),[9] indium gallium arsenide (InGaAs)[10,11] and mercury cadmium telluride (HgCdTe),[12] can realize a high performance in infrared band. But, the response for visible light of these detectors are extremely poor, which are limited by the short penetration length of visible light and low collection efficiency of photo-generated carriers. Compared with Si, Ge, InGaAs, or HgCdTe, the perovskite shows great potential in visible light response and many applications have been reported, such as solar cells[13–19] and photodetectors.[20–23] However, it is difficult to produce perovskite with narrow bandgap and its absorption cutoff wavelength can hardly extend longer than 1000 nm.[2–26] Therefore, a hybrid structure combining perovskite and traditional semiconductor materials is one of a promising alternative to realize a high performance broadband photodetector.

Previously, photodetector based on perovskite with Si,[27] Ge,[28] ZnO[29,30] or PbSe,[31] $CuInSe_2$,[32] have been successfully demonstrated, and the photo-response can be covered from about visible region to near infrared region.[33] A brief summary of comparison of various photodetectors is shown in Table S1 (Supporting Information). For example, a solution-processed, high-performance broadband (300–1100 nm) photodetectors based on double active layers incorporating narrow-bandgap $CuInSe_2$ (CISe) quantum dots (QDs) and halide perovskite are devised by Guo et al.[30] Previously, our group has demonstrated the organic-inorganic perovskite $MAPbI_3$/Ge heterojunction

Dr. H. Cong
State Key Laboratory for Supperlattices and Microstructures
Institute of Semiconductors
Chinese Academy of Science
Beijing 100083, P. R. China

Dr. X. Chu, Z. Chu, Prof. J. You
Key Laboratory of Semiconductor Materials Science
Institute of Semiconductors
Chinese Academy of Science
Beijing 100083, P. R. China

The ORCID identification number(s) for the author(s) of this article can be found under https://doi.org/10.1002/smtd.202100517.

DOI: 10.1002/smtd.202100517

F. Wan, X. Wang, Prof. C. Xue
State Key Laboratory on Integrated Optoelectronics
Institute of Semiconductors
Chinese Academy of Science
Beijing 100083, P. R. China
E-mail: clxue@semi.ac.cn

F. Wan, X. Wang, Prof. J. You, Prof. C. Xue
Center of Materials Science and Optoelectronics Engineering
University of Chinese Academy of Sciences
Beijing 100049, P. R. China

Y. Ma, J. Jiang, Prof. L. Shen
State Key Laboratory of Integrated Optoelectronics
College of Electronic Science and Engineering
Jilin University
Changchun 130012, P. R. China

photodetector, at an optical fiber communication wavelength of 1550 nm, the heterojunction device exhibits the highest responsivity of 1.4 A W^{-1}.[27] More recently, Geng et al constructed a fast response photodetector by integrating an organic-inorganic perovskite $MAPbBr_3$ with Si wafer, whose response range covered from 405 to 1064 nm.[26] However, there are still two parts could be further improved for these hybrid photodetectors. The first one is that photo-response range could be further extended, such as by using GeSn, which could extend the cutoff wavelength to 4 μm.[34] The second one is that the organic-inorganic hybrid perovskite could be substituted for the reason lacking of long term stability.

In this work, we demonstrated a broadband photodetector based on an inorganic perovskite $CsPbBr_3$/GeSn heterojunction. The detection range of the heterojunction device can be covered from 450 to 2200 nm. The visible light responsivity was enhanced by 4.92 times than that of a GeSn device under wavelength of 532 nm. The infrared band responsivity can also be raised, which is induced by the $CsPbBr_3$ film acting as anti-reflective coating. The responsivity for heterojunction detector was 1.42 times larger than that of GeSn one. In addition, the device with all inorganic components showed good stability. These results showed our inorganic perovskite/GeSn heterojunction device is of great potential in broadband photodetection with high responsivity.

2. Results and Discussion

The device structure of our $CsPbBr_3$/GeSn photodetector is shown in **Figure 1**a, inorganic perovskite was deposited on top of the GeSn film. $CsPbBr_3$ and GeSn layers were responsible for visible and infrared absorption, respectively. The GeSn film was grown on a 4-inch n-type Ge substrate using molecular beam epitaxy (MBE) system, according to the X-ray diffraction (XRD) result (Figure S1, Supporting Information), the Sn concentration was 7%. $CsPbBr_3$ layer was fabricated by solution method via spin coating subsequently. To verify the composition and quality of the prepared $CsPbBr_3$ film, XRD of $CsPbBr_3$ on GeSn was recorded, as shown in Figure S2 (Supporting Information). From the X-ray diffraction pattern of the $CsPbBr_3$ film on GeSn, we can see that all crystallographic signatures matched that of the pure $CsPbBr_3$ phase. The (100), (110), (200), and (210) and (202) reflections of the perovskite can be clearly observed respectively. X-ray photoelectron spectroscopy (XPS) of $CsPbBr_3$ on GeSn substrate has also been conducted, as depicted in Figure S3 (Supporting Information), the emission peak of Cs_{3d}, Pb_{4f}, Pb_{4d}, Br_{3d} can be clearly seen, from which we can confirm the existence of characteristic elements of $CsPbBr_3$. The front contact is semi-transparent Au electrode with a thickness of 20 nm. A bilayer of Ni/Au was deposited at the back of Ge substrate beforehand to form a good Ohmic contact. While the device working, the light was illuminated from the semitransparent Au side, as displayed in Figure 1a. In this configuration, the charges transport in vertical and the transition length in perovskite layer is about one hundred nanometers. The charge collection efficiency could be much better than the usually used lateral structure, where the charge need to transport in several micrometers.

According to the ultraviolet photoelectron spectroscopy (UPS) results of the $CsPbBr_3$ (Figure S3, Supporting Information), the band-alignment for each function layer can be drawn as Figure 1c, the details of carrier transfer process is explained later in the article. When the device is working, the $CsPbBr_3$ with wide-bandgap is contributed to the short wavelength absorption. The photo-generated electron-hole pairs can be separated under electrical field and electrons are collected by back-electrode through GeSn alloy without any barrier. The separation and collection process of photo carrier is highly efficient, which can be confirmed by photoluminescence (PL) measurement. As is shown in Figure 1d, when exited by 370 nm ultraviolet (UV) light, the PL emission of $CsPbBr_3$ film

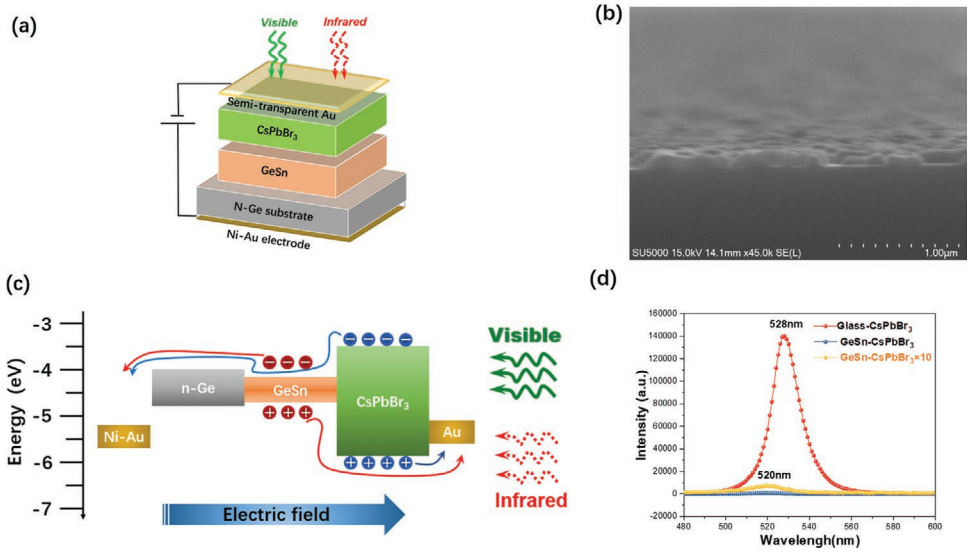

Figure 1. a) The schematic of the $CsPbBr_3$/GeSn heterojunction photodetector. b) Cross view scan electron microscopy (SEM) image of $CsPbBr_3$ deposited on GeSn film. c) Energy-band diagram for each functional material and carrier transfer process for visible light and infrared light. The vacuum energy is set as zero. d) PL spectrum for $CsPbBr_3$ spin-coated on glass and GeSn film.

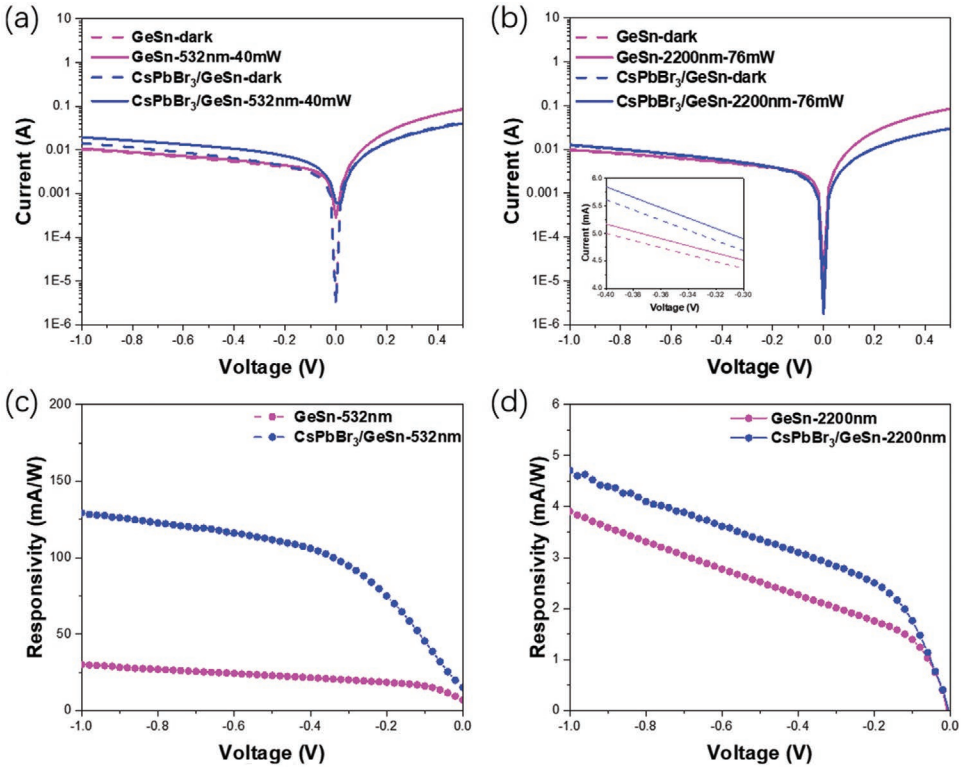

Figure 2. Optical response for both GeSn and $CsPbBr_3$/GeSn heterojunction devices. Dark current and photo current under normal incident light for wavelength of a) 532 nm, b) 2200 nm. Inset in (b): zoom-in graph for the reverse bias between 0.4 and 0.3 V. Responsivity versus voltage for c) 532 nm and d) 2200 nm.

on glass substrate was strong with a peak wavelength around 528 nm, corresponding to the band edge emission of $CsPbBr_3$ layer. When it comes to the $CsPbBr_3$ layer constructed on GeSn film, the PL intensity was almost quenched, suggesting that photo-generated charge can be efficiently extracted and separated at the $CsPbBr_3$/GeSn interface.

By taking the advantages of highly effective carrier transfer process, perovskite/GeSn heterojunction was used to build a broadband photodetector in this work, which covered a broadband response from visible light to SWIR. **Figure 2** shows the performance of this detector under vertical illuminance of different wavelengths. For comparison, a GeSn photodetector without perovskite layer was also fabricated. In Figure 2a, the dark current and photo current under 532 nm are shown for both of heterojunction and GeSn device (device area 0.5 cm^2). The calculated dark current density are 20 and 28 mA cm^{-2} for GeSn and $CsPbBr_3$/GeSn photodetector at reverse bias of 1 V. Dark current is one of the extremely crucial parameters for photodetector, as it can be influenced by many elements, such as material bandgap, defects, operating temperature, and so on. For an ideal p-n junction, the reversed dark current (J_s) can be defined by the following relations:

$$J_s \propto T^{\frac{3}{2}} \exp\left(-\frac{E_g}{k_0 T}\right) \exp\left(\frac{qV}{k_0 T}\right) \quad (1)$$

where T is the temperature, E_g is the material bandgap and k_0 is the Boltzmann constant, q is the elementary charge. From the equation above, we can see that the while the bandgap is smaller, the dark current will be increased. As the bandgap of GeSn we adopted is 0.55 eV, which is a quite narrow bandgap semiconductor, this can increase the device dark current compared with other detectors operated in the range of visible light. In addition, growth of high quality GeSn film on Ge substrate is still a challenge at present. The defects and dislocations in GeSn film lead to the carrier recombination and increase the dark current, which are mainly caused by lattice mismatching between GeSn and Ge, it could be decreased by optimized the growing conditions.

The photocurrent is generated under a normally incident light from 532 nm laser with power of 40 mW. The calculated responsivity (R) values are shown in Figure 2c. The R value is 129 mA W^{-1} for the heterojunction device, which is nearly 4.3 times larger than that of GeSn device. Moreover, the responsivity is much higher than recent reports on the perovskite/Si photodetector (≈10 mA W^{-1}).[26] To characterize the device performance in the range of SWIR, photo response was measured using a laser with the wavelength of 2200 nm and power of 76 mW. The dark and light currents are shown in Figure 2b, the calculated responsivity versus voltage is plot in Figure 2d. Taking the Sn concentration and strain into consideration, the bandgap of GeSn alloy is 0.55 eV corresponding to a cutoff wavelength of 2250 nm.[35,36] Enhancement of responsivity can be achieved for the device with perovskite constructed on GeSn film.

To further characterize the device performance, we also measure the photo response for wavelength of 450 and 1550 nm, the current versus voltage curves are shown in supporting information (Figure S4, Supporting Information).

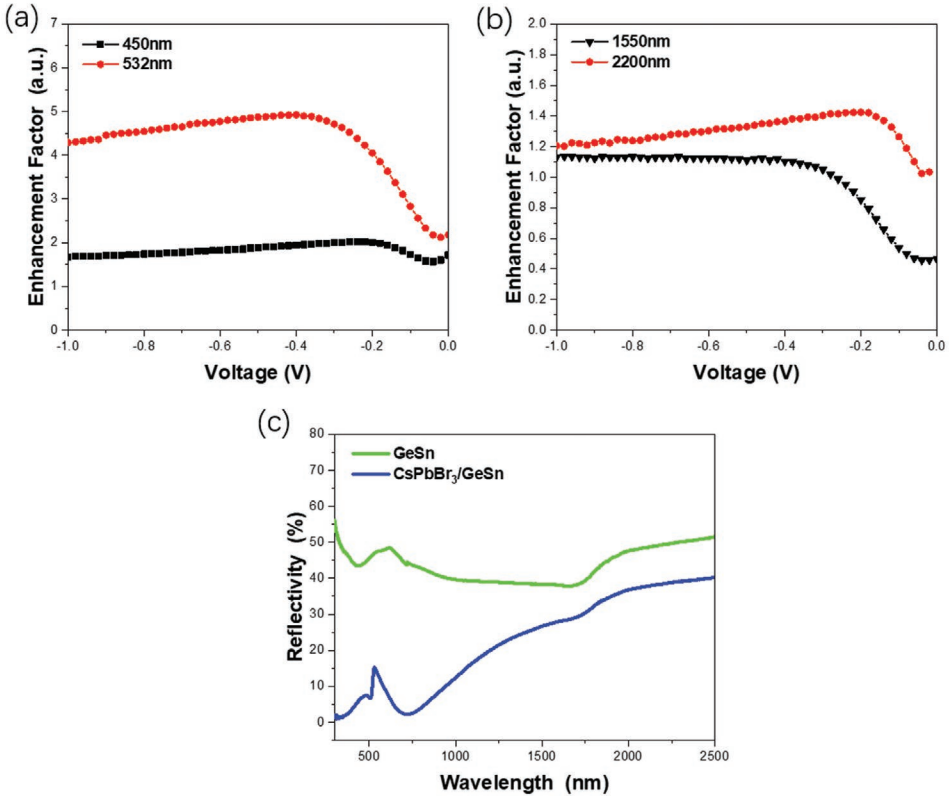

Figure 3. Calculated enhancement factor versus voltage for a) visible light (450 and 532 nm) and b) infrared light (1550 and 2200 nm). c) Measured reflectivity for GeSn film and $CsPbBr_3$/GeSn heterojunction.

Figure 3a shows the calculated enhancement factors (EFs) under visible light illumination, where the EF is defined as the ratio between responsivity for $CsPbBr_3$/GeSn heterojunction and GeSn device. The increased photo response in visible is mainly caused by the high absorption efficiency of perovskite film. The enhancement factor can achieve 4.92 and 2.02 for wavelength of 532 and 450 nm, respectively. As is shown in Figure 3b, the enhancement factor for 1550 nm increased with applied bias voltage and reached a saturation value of 1.13 under bias of –0.4 V. As the photons are absorbed by GeSn alloy and highly doped Ge substrate, carrier recombination process played a leading role at low reverse bias, which could be the reason of no responsivity enhancement observed while applying the bias less than –0.4 V. Moreover, extra energy is also required for holes transfer through the high barrier from GeSn to perovskite. Similar process can be found in 2200 nm absorption. As the photon absorption only takes place in undoped GeSn film, the enhancement can be achieved under low bias. The maximum enhancement is 1.42 for 2200 nm under bias of –0.2 V. As the refractive index of GeSn (Ge) is measured to be 4.3 (4.25) at the wavelength of 1550 nm.[37] Perovskite film works as an anti-reflection coating for GeSn film with a reflective index of 1.59 measured using ellipsometer. The n-k relations for $CsPbBr_3$ is shown in Figure S5 (Supporting Information). Compared with the pristine GeSn film, the decrease of reflectivity for heterojunction is shown in Figure 3c, which maybe one of the reasons for the photo-response enhancement around 2200 nm.

We measured the light on/off frequency response characteristic of perovskite/GeSn photodetector by the transit photo current. From the time response under a 5 Hz pulse at the wavelength of 532 nm (**Figure 4**), the fall time can be estimated to be 26 µs at reverse bias of –2 V, which is comparable of the single crystal of perovskite (15.8 µs).[38] We also tested the frequency response characteristic of the GeSn device, the response time

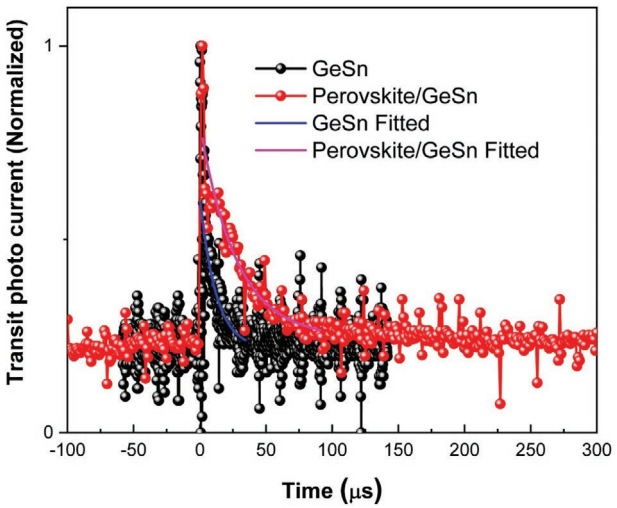

Figure 4. Photo-response time measured by the transit photo-current method.

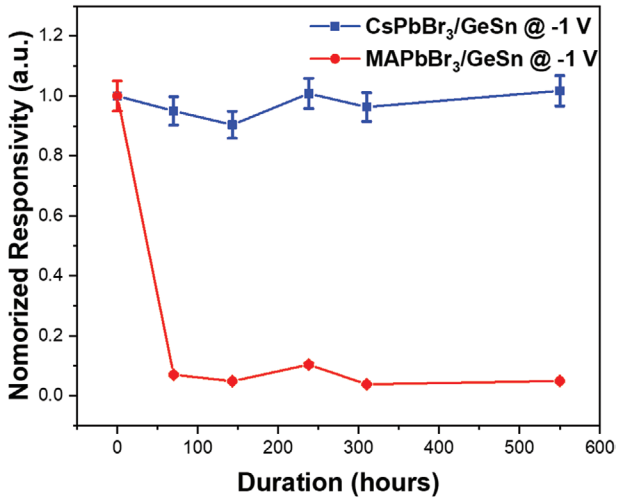

Figure 5. Normalized responsivity for $CsPbBr_3$/GeSn and $MAPbBr_3$/GeSn devices as a function of storage time in dry glove box.

is 12 µs. Generally, for the GeSn based photodetector, the response time should be in nano-second,[39] the slow response could be due to the large area of the device (0.5 cm^2) because of the limitation of resistance-capacitance (RC) time constant.[40] This could be improved by design small area of the devices in the future.

Stability is critical for halide perovskite based optoelectronic devices, we monitored the stability of the $CsPbBr_3$/GeSn heterojunction in the dry glove box. For comparison, the stability of the organic/inorganic hybrid $MAPbBr_3$ with the GeSn heterojunction is also collected. The normalized responsivity for these devices are shown in **Figure 5**, for the inorganic perovskite $CsPbBr_3$ combined with GeSn, the device can almost keep its original responsivity over than 550 h. While, the device utilizing the organic/inorganic hybrid perovskite can only survive for several 10 h. This result definitely showed the advantage of the all inorganic $CsPbBr_3$/GeSn heterojunction in the stability.

3. Conclusion

In conclusion, we demonstrated an all inorganic $CsPbBr_3$/GeSn heterojunction based photodetector, which can be used for broadband detection in the wavelength ranged from 450 to 2200 nm. An obvious enhancement of photo-response in visible region has been observed compared with the GeSn based device. In addition, the device showed a fast response time even though the device is still large. Moreover, the device can almost sustain its original performance while keeping for over than 500 h. These results demonstrated that the perovskite/GeSn heterojunction could be very promising in broadband detection and high speed imaging.

4. Experimental Section

Epitaxy of GeSn Alloy: The 200 nm-thick GeSn alloy was grown on a n-type 4-inch Ge wafer using molecular beam epitaxy system, the resistance of substrate was $2.1 \pm 0.3 \times 10^{-2}$ Ω cm. The Ge substrate was cleaned using dilute HF and de-gas for 5 h under temperature of 120 °C. The used de-oxygen temperature was set at 450 °C and the GeSn alloy was grown at 160 °C.

$CsPbBr_3$ Film Deposition: CsBr (Sigma Aldrich, 99.9%) and $PbBr_2$ (Sigma Aldrich, 99.99%) were used to prepare precursor solutions. The molar ratio CsBr: $PbBr_2$ was 2:1 using DMSO as a solvent. The solution concentration was 0.5 M (CsBr 1 M, $PbBr_2$ 0.5 M). A high ratio of CsBr: $PbBr_2$ was used to suppress the formation of non-$CsPbBr_3$ phases. The precursor solutions were stirred at 45 °C overnight. And then the solution was stand for 4 h at room temperature, precipitates were formed in the CsBr-rich solution, top transparent solution was decanted and filtered for using. This was consistent with the previous experimental details while using $CsPbBr_3$ in the light-emitting diodes.[41]

Device Fabrication: GeSn or glass substrate was first cleaned by sonication using deionized water, acetone, and isopropanol in sequence for 20 min each and then treated in a UV ozone cleaner for 20 min. Then, the perovskite precursor (CsBr:$PbBr_2$ = 2:1) was spin-coated onto GeSn epitaxial wafer or glass substrate at 2000 rpm for 90 s, and annealed at 80 °C for 20 min. Next, 20 nm Au metal electrodes were deposited by thermal evaporation on top of the as-prepared $CsPbBr_3$ film or GeSn substrate as target photodetectors or the control one respectively.

Material and Device Characterization: The morphologies of perovskite and also the half-completed devices were characterized by scan electron microscopy SEM (Hitachi SU5000). The PL spectrum measurements were carried out by FLS980 Spectrometer utilizing 375 nm wavelength light separated from Xe lamb as excitation. The Sn concentration was determined by XRD (PANalytical X'Pert^3 MRD) and the crystallinity of $CsPbBr_3$ was confirmed using XRD on a Rigaku D/MAX-2500 system using Cu Kα radiation. The reflectivity spectrum was measured using Agilent Cary Series VU–vis-NIR spectrophotometer. Ultraviolet photoelectron spectroscopy (UPS) spectra were carried out on a Thermo Scientific ESCALab 250Xi using HeI (21.22 eV) radiation lines. The *I–V* curves were recorded by a KEYSIGHT B1500A Semiconductor Device Analyzer. Two lasers (450 and 532 nm) were used as visible light source, another two lasers (1550 and 2200 nm) were used as IR source. The measurement of the response speed was carried out by the transient photocurrent (TPC) method. The optical pump was set at the wavelength of 532 nm with spot size of 5 mm^2. And the light source was operated with pulse width of 10 ns at the repetition rate of 4–5 Hz. The photodetectors collected the pulsed light signal emitted by the pulsed laser, then a 2.5 GHz oscilloscope (KEYSIGHT InfiniiVision DSOX6004A) recorded the current pulse and generated the corresponding TPC curve. The response speed could be defined as the photocurrent decay time from the peak down to approximately 1/e after a single exponential fit to the TPC curve. For the stability test, the devices were stored in the nitrogen glove box, and the devices were taken out in the ambient air for testing.

Supporting Information

Supporting Information is available from the Wiley Online Library or from the author.

Acknowledgements

H.C. and X.C. contributed equally to this work. This work was supported by the National Natural Science Foundation of China (Grant No. 61874109), Key Research Program of Frontier Sciences (Grant No. ZDBS-LY- JSC008).

Conflict of Interest

The authors declare no conflict of interest.

Data Availability Statement

The data that supports the findings of this study are available in the supplementary material of this article.

Keywords

all-inorganic perovskites, broadband photodetector, $CsPbBr_3$/GeSn heterojunctions, germanium tin, vertical device structures

Received: May 13, 2021
Revised: June 4, 2021
Published online: June 23, 2021

[1] L. Li, H. Chen, Z. Fang, X. Meng, C. Zuo, M. Lv, Y. Tian, Y. Fang, Z. Xiao, C. Shan, Z. Xiao, Z. Jin, G. Shen, L. Shen, L. Ding, *Adv. Mater.* **2020**, *32*, 1907257.
[2] X. Tang, M. M. Ackerman, M. Chen, P. Guyot-Sionnest, *Nat. Photonics* **2019**, *13*, 277.
[3] V. Krishnamurthi, H. Khan, T. Ahmed, A. Zavabeti, S. A. Tawfik, S. K. Jain, M. J. S. Spencer, S. Balendhran, K. B. Crozier, Z. Li, L. Fu, M. Mohiuddin, M. X. Low, B. Shabbir, A. Boes, A. Mitchell, C. F. McConville, Y. Li, K. Kalantar-Zadeh, N. Mahmood, S. Walia, *Adv. Mater.* **2020**, *32*, 2004247.
[4] H. Lu, G. M. Carroll, N. R. Neale, M. C. Beard, *ACS Nano* **2019**, *13*, 939.
[5] P. Luo, F. Wang, J. Qu, K. Liu, X. Hu, K. Liu, T. Zhai, *Adv. Funct. Mater.* **2020**, *31*, 2008351.
[6] L. H. Zeng, Q. M. Chen, Z. X. Zhang, D. Wu, H. Y. Yuan, Y. Y. Li, W. Qarony, S. P. Lau, L. B. Luo, Y. H. Tsang, *Adv. Sci.* **2019**, *6*, 1901134.
[7] Y. J. Dai, X. F. Wang, W. B. Peng, C. Xu, C. S. Wu, K. Dong, R. Y. Liu, Z. L. Wang, *Adv. Mater.* **2018**, *30*, 1705893.
[8] Z. Huang, J. E. Carey, M. Liu, X. Guo, E. Mazur, J. C. Campbell, *Appl. Phys. Lett.* **2006**, *89*, 033506.
[9] M. Oehme, M. Kaschel, J. Werner, O. Kirfel, M. Schmid, B. Bahouchi, E. Kasper, J. Schulze, *J. Electrochem. Soc.* **2010**, *157*, H144.
[10] A. Rogalski, *Infrared Detectors*, CRC Press, USA **2010**.
[11] P. A. Hiskett, G. S. Buller, A. Y. Loudon, J. M. Smith, I. Gontijo, A. C. Walker, P. D. Townsend, M. J. Robertson, *Appl. Opt.* **2000**, *36*, 6818.
[12] A. Rogalski, J. Antoszewski, L. Faraone, *J. Appl. Phys.* **2009**, *105*, 091101.
[13] K. Xiao, R. Lin, Q. Han, Y. Hou, Z. Qin, H. T. Nguyen, J. Wen, M. Wei, V. Yeddu, M. I. Saidaminov, Y. Gao, X. Luo, Y. Wang, H. Gao, C. Zhang, J. Xu, J. Zhu, E. H. Sargent, H. Tan, *Nat. Energy* **2020**, *5*, 870.
[14] J. Y. Kim, J.-W. Lee, H. S. Jung, H. Shin, N.-G. Park, *Chem. Rev.* **2020**, *120*, 7867.
[15] M. Jeong, I. W. Choi, E. M. Go, Y. Cho, M. Kim, B. Lee, S. Jeong, Y. Jo, H. W. Choi, J. Lee, J.-H. Bae, S. K. Kwak, D. S. Kim, C. Yang, *Science* **2020**, *369*, 1615.
[16] Q. Jiang, Y. Zhao, X. Zhang, X. Yang, Y. Chen, Z. Chu, Q. Ye, X. Li, Z. Yin, J. You, *Nat. Photonics* **2019**, *13*, 460.
[17] Q. Ye, Y. Zhao, S. Mu, F. Ma, F. Gao, Z. Chu, Z. Yin, P. Gao, X. Zhang, J. You, *Adv. Mater.* **2019**, *31*, 1905143.
[18] F. Gao, Y. Zhao, X. W. Zhang, J. B. You, *Adv. Energy Mater.* **2020**, *10*, 1902650.
[19] W. C. Xiang, W. Tress, *Adv. Mater.* **2019**, *31*, 1902851.
[20] L. T. Dou, Y. Yang, J. B. You, Z. R. Hong, W. H. Chang, G. Li, Y. Yang, *Nat. Commun.* **2014**, *5*, 5404.
[21] M. Ahmadi, T. Wu, B. Hu, *Adv. Mater.* **2017**, *29*, 1605242.
[22] C. Xie, C. K. Liu, H. L. Loi, F. Yan, *Adv. Funct. Mater.* **2019**, *30*, 1903907.
[23] H. Gu, S.-C. Chen, Q. Zheng, *Adv. Opt. Mater.* **2020**, *9*, 2001637.
[24] C. K. Liu, Q. D. Tai, N. X. Wang, G. Q. Tang, H. L. Loi, F. Yan, *Adv. Sci.* **2019**, *6*, 1900751.
[25] W. Wang, D. Zhao, F. Zhang, L. Li, M. Du, C. Wang, Y. Yu, Q. Huang, M. Zhang, L. Li, J. Miao, Z. Lou, G. Shen, Y. Fang, Y. Yan, *Adv. Funct. Mater.* **2017**, *27*, 1703953.
[26] F. Cao, W. Tian, M. Wang, L. Li, *InfoMat* **2020**, *2*, 3.
[27] X. Geng, F. Wang, H. Tian, Q. Feng, H. Zhang, R. Liang, Y. Shen, Z. Ju, G.-Y. Gou, N. Deng, Y.-t. Li, J. Ren, D. Xie, Y. Yang, T.-L. Ren, *ACS Nano* **2020**, *14*, 2860.
[28] W. Hu, H. Cong, W. Huang, Y. Huang, L. Chen, A. Pan, C. Xue, *Light: Sci. Appl.* **2019**, *8*, 106.
[29] S. Liu, X. Liu, Z. Zhu, S. Wang, Y. Gu, F. Shan, Y. Zou, *Mater. Res. Bull.* **2020**, *130*, 110956.
[30] H. Wang, P. Zhang, Z. Zang, *Appl. Phys. Lett.* **2020**, *16*, 116.
[31] T. Zhu, Y. Yang, L. Zheng, L. Liu, M. L. Becker, X. Gong, *Adv. Funct. Mater.* **2020**, *30*, 1909487.
[32] R. Guo, C. Bao, F. Gao, J. Tian, *Adv. Opt. Mater.* **2020**, *8*, 2000557.
[33] P. Zhu, J. Zhu, *InfoMat* **2020**, *2*, 2.
[34] M. Atalla, S. Assali, A. Attiaoui, C. Leduc, A. Kumar, S. Abdi, O. Moutanabbir, *Adv. Funct. Mater.* **2020**, 2006329.
[35] H. Cong, C. Xue, J. Zheng, F. Yang, K. Yu, Z. Liu, X. Zhang, B. Cheng, Q. Wang, *IEEE Photonics J.* **2016**, *8*, 1.
[36] H. Cong, F. Yang, C. Xue, K. Yu, L. Zhou, N. Wang, B. Cheng, Q. Wang, *Small* **2018**, *14*, 1704414.
[37] H. Tran, W. Du, S. A. Ghetmiri, A. Mosleh, G. Sun, R. A. Soref, J. Margetis, J. Tolle, B. Li, H. A. Naseem, S. Yu, *J. Appl. Phys.* **2016**, *119*, 103106.
[38] Y. Liu, Y. Zhang, Z. Yang, J. Feng, Z. Xu, Q. Li, M. Hu, H. Ye, X. Zhang, M. Liu, K. Zhao, S. Liu, *Mater. Today* **2019**, *22*, 67.
[39] X. Li, L. Peng, Z. Liu, Z. Zhou, J. Zheng, C. Xue, Y. Zuo, B. Chen, B. Cheng, *Photonic Res.* **2021**, *9*, 494.
[40] Y. Zhao, C. Li, L. Shen, *InfoMat* **2019**, *1*, 407.
[41] L. Zhang, X. Yang, Q. Jiang, P. Wang, Z. Yin, X. Zhang, H. Tan, Y. Yang, M. Wei, B. R. Sutherland, E. H. Sargent, J. You, *Nat. Commun.* **2017**, *8*, 15640.